ESR Imaging of Tracer Translational Diffusion in Polystyrene Solutions and Swollen Networks

Zhan Gao, Jan Pilař,† and Shulamith Schlick*

Department of Chemistry, University of Detroit Mercy, Detroit, Michigan 48219

Received: November 28, 1995; In Final Form: March 6, 1996[⊗]

The translational diffusion coefficients of a small paramagnetic molecule (the deuteriated nitroxide PDTEMPONE) as tracer were measured in solutions of polystyrene (PS) in toluene and dimethylformamide (DMF) and in cross-linked polystyrene (cPS) networks swollen by the same solvents, using two-dimensional spatial−spectral electron spin resonance imaging (2D ESRI). PS solutions containing 30, 40, and 50 w/w % polymer were examined in toluene at 300, 305, 310, and 315 K and in DMF at 300 K. PS networks prepared with 0.5, 1.0, 2.5, and 5.0 mol % divinylbenzene as cross-linker were swollen in toluene or DMF and studied at 300 K. Two-dimensional images describing the distribution of the diffusant in the sample were reconstructed from a complete set of projections obtained as a function of the magnetic field gradient applied along the symmetry axis of the sample. The concentration profile of the diffusant at a given time was obtained by integrating absorption ESR spectra in slices perpendicular to the spatial axis, which was divided into 256 points. These profiles were obtained as a function of time, and the diffusion coefficients were determined by simulating the experimental diffusion profiles using Fick's model of diffusion. The diffusion coefficients were found to depend on the solvent, temperature, and PS concentration in the solutions and are significantly reduced by cross-linking in the swollen networks. The temperature dependence of the diffusion coefficients shows an Arrhenius behavior, and their dependence on the polymer concentration in the solutions is consistent with the free volume theory. Results from this study were compared with those obtained for solvent self-diffusion and diffusion of other tracers in PS solutions and swollen networks.

Introduction

Data on transport properties in bulk polymers, polymer solutions, and swollen polymer networks are of considerable importance in the modeling of polymer dynamics and in numerous practical applications.[1−4] The applications include electrophoresis, chromatography, enhanced oil recovery, polymerization kinetics, coatings, drug delivery systems, and catalytic processes on polymer supports. The fundamental importance of transport studies is in the ability to examine quantitatively the interaction between polymer, solvent, and various guests and to describe relaxation phenomena in the presence of temporary entanglements in polymer solutions and obstacles such as permanent cross-links in polymer networks.

Numerous recent papers on diffusion processes in polymeric systems have focused on the study of self-diffusion of solvents and polymers and on the diffusion of monomeric, oligomeric, and polymeric tracers in polymer solutions and swollen networks.[5−13] The diffusion coefficient D and viscosity η have been measured as a function of the molecular mass of the diffusant M, the polymer concentration c, the molecular mass between cross-links M_x, and the temperature; the results have been compared with the predictions of various models. Of great interest is the crossover of the diffusion behavior from the Stokes−Einstein model for low molecular mass diffusants ($D \sim M^{-0.5}$ in a Θ solvent and $D \sim M^{-0.6}$ in a good solvent) to the prediction of the reptation theory[14] for polymeric diffusants ($D \sim M^{-2}$ for self-diffusion and $D \sim M^{-1.8}$ when the diffusant and matrix are chemically different polymers).

The time-dependent local concentration of diffusing species in polymeric systems has been measured by chemical, optical, and radioactive tracers, dynamic light scattering (DLS), fluorescence photobleaching recovery (FPR), and spectroscopic methods.[5,8−13] DLS has been used extensively for the study of polymers in organic solvents. The study of aqueous polymer systems, which are becoming increasingly important due to environmental and health concerns, presents additional problems, because of the difficulty to match the index of refraction of the solvent to that of the matrix. For many aqueous systems, pulsed field-gradient spin echo (PFGSE) NMR has emerged as the dominant method. Some of the difficulties expected in the application of this technique have been recently discussed.[15−18] Critical review of the literature reveals problems associated with the accuracy of most methods for measuring diffusion coefficients, and differences of 20−30% are common even for identical experiments.[11,13]

The effect of paramagnetic species on the nuclear spin−lattice relaxation time T_1 is the basis of a recent elegant method for the measurement of diffusion of paramagnetic species such as Cu^{2+} and nitroxide spin probes in aqueous gels by NMR imaging (NMRI).[19] NMRI has been used to study sorption processes and provides an image of the NMR signal as a function of spatial coordinates, in one, two, and three dimensions.[20−22] These studies have made possible the visualization of motional and structural heterogeneities in cross-linked elastomers and other materials. To the best of our knowledge, however, such studies have not provided quantitative evaluation of diffusion coefficients.

Electron spin resonance imaging (ESRI) can supply information on the spatial distribution of paramagnetic molecules in a sample and has been used successfully for measurements of translational diffusion.[23−25] Diffusion coefficients of paramagnetic diffusants can be deduced from an analysis of the time

* To whom correspondence should be addressed. e-mail SCHLICKS@UDMERCY.EDU.

† On leave from the Institute of Macromolecular Chemistry (IMC), Academy of Sciences of the Czech Republic, 162 06 Prague 6, Czech Republic.

⊗ Abstract published in *Advance ACS Abstracts,* May 1, 1996.

S0022-3654(95)03507-6 CCC: $12.00

dependence of concentration profiles along a selected axis of the sample. The determination of diffusion coefficients of spin probes in liquid crystals and model membranes has been described in a series of papers by Freed and co-workers.[26−28] Recent improvements in the technique of dynamic imaging of diffusion by ESR have allowed the measurement of diffusion coefficients of the order of 10^{-7} cm^2 s^{-1} in 1 h.[27]

In our laboratory, ESRI in two dimensions (spectral−spatial) is developed and used for real-time representations of structural inhomogeneities and dynamics in polymer blends, ionomers, composites, and cross-linked polymer gels.[29−31] Projections of the sample measured in a range of magnetic field gradients applied along the spatial axis are used to reconstruct a 2D spectral−spatial image, which consists of a sequence of absorption ESR spectra of the paramagnetic molecules located in planes perpendicular to the spatial axis. The method requires long measurement times but can supply not only the concentration profile of the diffusant but also the ESR line shapes of the diffusant in each slice of the sample perpendicular to the direction of the diffusion. This approach makes possible determination of the translational diffusion along the spatial axis of the sample and of the microscopic rotational diffusion of the diffusant in the same experiment. The application of this method to the study of diffusion processes in polymer hydrogels has been published recently.[31]

We present the application of 2D ESRI to measuring the translational diffusion of a small nitroxide spin probe in PS solutions and in cross-linked polystyrene (cPS) networks as a function of polymer concentration, degree of cross-linking, temperature, and solvent. The study was initiated in order to assess the effect of the swelling solvent on the diffusion rates of small neutral diffusants, to compare transport properties of the exogenous tracer to those of the solvent, and to compare diffusion processes in polymer solutions and in the corresponding swollen networks. On the basis of the results presented below, it appears that the development of 2D ESRI is important for the evaluation of the transport properties of materials suitable in medical and industrial applications.

Experimental Section

Linear Polystyrene. Toluene and DMF (Fisher) were distilled before use. Solutions containing 30, 40, and 50 w/w % polystyrene (PS) (Aldrich, MW = 2.8×10^5, T_g = 373 K, density = 1.046 g/mL) in toluene and DMF were prepared by mixing the proper amounts of PS and solvent. The mixtures were kept at ambient temperature for 1 week to ensure complete dissolution of the polymer. The notation used for these solutions is PS30, PS40, and PS50.

Cross-Linked Polystyrene. A series of cross-linked PS (cPS) samples were prepared by bulk polymerization. Styrene (Aldrich) was washed three times with 10% aqueous NaOH solution and then with water, to a pH close to 7. The washed monomer was mixed with the cross-linker divinylbenzene (DVB, Aldrich, 55 w/w % *p*- and *m*-divinylbenzene, 45 w/w % *p*- and *m*-diethylbenzene) and with benzoyl peroxide (Baker, 99% pure) as initiator; the weight of the initiator was ≈10% of the total monomer weight. The cross-linker concentration was 0.5, 1.0, 2.0, 2.5, and 5.0, in mol % DVB. The polymerization took place in capillaries 1.5−1.8 mm o.d. and 100 mm long in an oil bath; the temperature of the bath was increased gradually at a rate of 5 K/min to 373 K and then kept constant at 373 K for 24 h. The notation used for these cross-linked systems is cPS05, cPS10, cPS20, cPS25, and cPS50. The calculated average molecular mass between cross-links based on the DVB content, $M_{x,\,\mathrm{stoich}}$, is given in Table 1.

TABLE 1: Diffusion Coefficients (*D*) of PDTEMPONE in Polystyrene Solutions and Swollen Polystyrene Networks

	w_2 (w/w %)		D (10^{-6} cm^2 s^{-1}) in toluene				D (10^{-6} cm^2 s^{-1}) in DMF	
sample	toluene	DMF	300 K	305 K	310 K	315 K	300 K	$M_{x,\mathrm{stoich}}$
PS30	30	30	4.0	7.3	9.0	≥10	6.9	
PS40	40	40	1.8	2.5	3.2	4.5	4.4	
PS50	50	50	0.8	1.3	1.8	2.5		
cPS05		22					1.9	10400
cPS10	14.9	40	3.4				1.3	5200
cPS20	17.6		2.3					2600
cPS25	18.0		1.7					2080
cPS50	28.5		0.4					1040

After polymerization, the glass capillaries were removed, and the exposed cPS rods, typically 1 cm in length, were swollen to equilibrium at ambient temperature for a minimum of 10 days in the presence of excess solvent. The swelling factors (weight percent of the solvent in the swollen networks) were determined gravimetrically. The polymer content in the swollen network, calculated from the swelling factors and expressed by w_2 values (w/w %), is also given in Table 1. The swelling factor for cPS is higher in toluene than in DMF and decreases with increasing cross-linking density in both solvents.

Diffusant. The nitroxide free radical perdeuterio-2,2′,6,6′-tetramethyl-4-piperidone-*N*-oxyl (PDTEMPONE, MW 170) was synthesized according to the literature[32] and used as the paramagnetic diffusant. Stock solutions of this nitroxide (≈0.1 mol/L) in the pure solvents and in the PS solutions in toluene and DMF were prepared.

Sample Preparation. For imaging experiments of PS solutions, cylindrical sample tubes (3 mm o.d., 12 mm length) were used. After sealing of one end, the sample tube was filled with the stock PS solution to a maximum length of 9 mm and topped with a layer of thickness h (≈1 mm) of the same PS solution, which also contained the diffusant PDTEMPONE. The tubes were flame-sealed inside a thin wall Pyrex sample tube (5 mm o.d.) and positioned vertically in the cavity of the ESRI spectrometer, with the layer containing PDTEMPONE on top. Diffusion processes were measured at 300, 305, 310, and 315 K for toluene as solvent and at 300 K for DMF as solvent.

For imaging of the cPS samples, swelling was carried out in capillary sections ≈10 mm long, cut from the longer tubes containing the bulk polymer. After swelling, samples that contained no cracks or bubbles were selected after removing the extra gel outside the tube, and the length was adjusted to ≈8 mm; next, ≈1 mm of the glass tube was removed at one end, and the exposed gel portion was soaked for 5−10 min at ambient temperature with the solution of PDTEMPONE in the same swelling solvent. The samples were immediately flame-sealed inside thin wall Pyrex sample tubes (3−4 mm o.d.) and positioned in the ESR cavity as described for the PS solutions. Diffusion processes were measured at 300 K.

ESRI Measurements. The ESR imaging system in Detroit is based on the Bruker 200D ESR spectrometer and is equipped with two Lewis coils (George Associates, Berkeley, CA, Type 503D) that supply a maximum linear gradient of 320 G/cm in the direction parallel to the external magnetic field or 250 G/cm in the vertical direction. The spectrometer is interfaced to a 386 AST PC equipped with software designed to control the magnitude of the field gradient and to collect data. The raw data were processed, and the diffusion profiles were simulated with a NEC READY 486 PC. Additional details have been published.[31]

The progress of diffusion was followed from spatial−spectral images measured as a function of time. Each image was

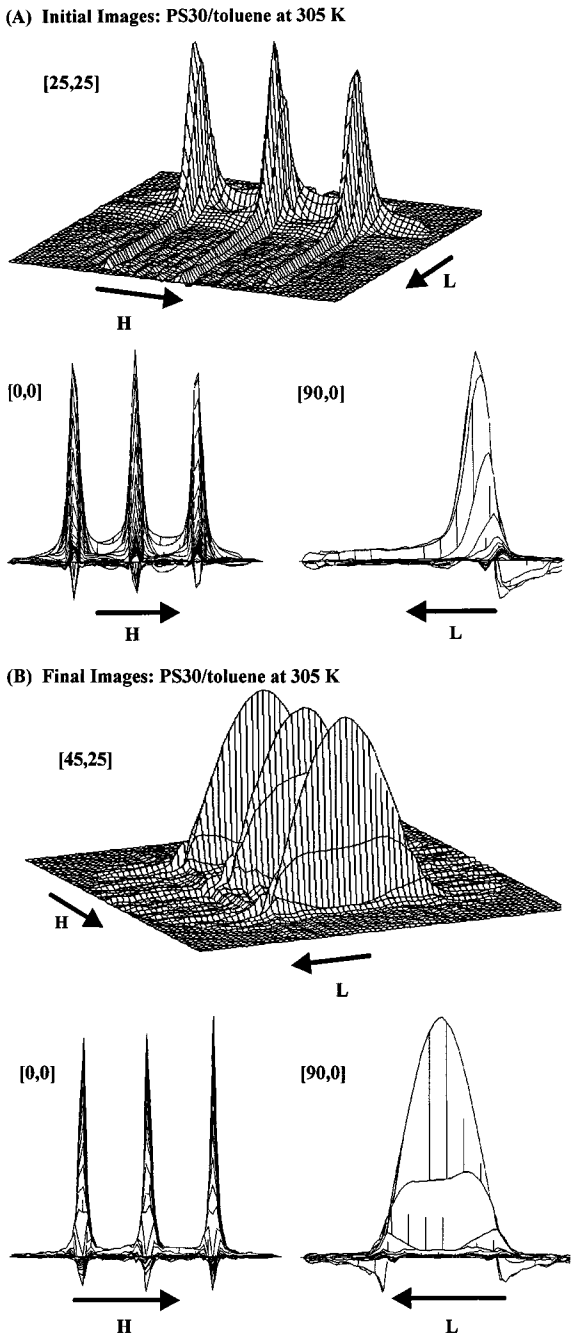

Figure 1. Perspective plots of the initial (A) and final (B) images for the diffusion of PDTEMPONE in PS30/toluene at 305 K and the corresponding images in the spatial (*L*) and spectral (*H*) axes. The viewing angles in the θ and ϕ in the *L* (spatial), *I* (intensity), and *H* (spectral) axes are given in square brackets for all plots.

reconstructed from a complete set of projections taken as a function of the magnetic field gradient,[33,34] using a convoluted back-projection algorithm.[29] The number of points for each projection (4096) was kept constant. The maximum magnetic field gradient G_{max}, spectral width ΔH, and sample length l determine the maximum experimentally accessible projection angle α_{max} ($\tan \alpha_{max} = (l/\Delta H)G_{max}$) and the maximum sweep width SW_{max} ($SW_{max} = \sqrt{2}\Delta H/\cos \alpha_{max}$). For $\Delta H = 42$G, which was broad enough for the motionally narrowed ESR spectrum of PDTEMPONE, sample length $l = 1.2$ cm, and $G_{max} = 175$ G/cm along the vertical axis, we obtain $\alpha_{max} = 78.7°$ and $SW_{max} = 304.5$ G. A complete set of data for one image consisted of 65 projections, taken for gradients corresponding to equally spaced increments of α in the range $-90°$ to $+90°$;

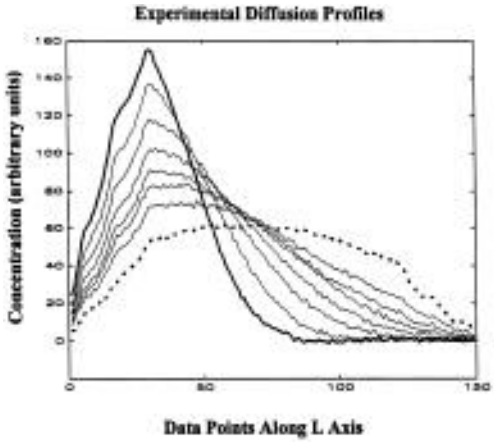

Figure 2. Experimental concentration profiles for the diffusion of PDTEMPONE in PS30 at 305 K. Consecutive images were taken at t = 5, 33, 67, 113, 167, 213, 303, and 1565 min. The abscissa is the number of points corresponding to the actual length of the sample, out of a total of 256 points collected.

of these projections, 57 are experimentally accessible projections and eight are projections at missing angles (for α in the intervals from α_{max} to 90° and from $-\alpha_{max}$ to $-90°$). The projections at the missing angles were assumed to be the same as those at the maximum or minimum experimentally accessible angles $\pm\alpha_{max}$, respectively. Even when an acceptable signal-to-noise ratio was reached after one scan (scan time 10 s, microwave power 2 mW, modulation 1 G, time constant 10 ms), the acquisition of the projections necessary for each image at a given time t required $\approx$30 min. These conditions imply that the method can be used for the study of relatively slow diffusion processes, when the change of the concentration profile during acquisition time is negligible. The concentration of the diffusant at each point of the spatial axis of a sample was obtained by integrating the ESR spectra at this point along the spectral (magnetic field) axis, thus providing the corresponding experimental concentration profile at time t.

Results and Discussion

In Figure 1 we present typical data obtained in ESRI experiments. Figure 1A (top) shows the initial image as a perspective plot in the spectral−spatial−intensity axes for the diffusion of PDTEMPONE in PS30/toluene at 305 K, together with the spectral (along *H*) and spatial (along *L*) views (bottom). Figure 1B presents the corresponding plots for the final image. In all plots we have indicated in square brackets the viewing angles θ and ϕ in the axes system *L* (spatial), *I* (intensity), and *H* (spectral) coordinates. The broader spectral lines clearly seen in the initial spectral image (Figure 1A, bottom left) are due to the high initial concentration of spin probes in the top layer of the sample. The resolution in the spectral plots is limited by the number of points (256). For this reason the amplitude ratios in the spectral image of Figure 1B are not as expected for motionally averaged nitroxide signals. Details on the spectral line shapes are obtained from the integrated spectra, which contain 4K points.

A complete series of experimental concentration profiles as a function of time for the diffusion of PDTEMPONE at 305 K in PS30/toluene are presented in Figure 2. The final concentration profile, which is used for normalizing the simulated profiles for cavity sensitivity along the diffusion direction, is shown by dashed lines. The part of the profiles corresponding to the sample length (as shown in Figure 2) was splined using a cubic spline with 16 equidistant control points. The experimental splined concentration profiles in the *L* scale generated in this

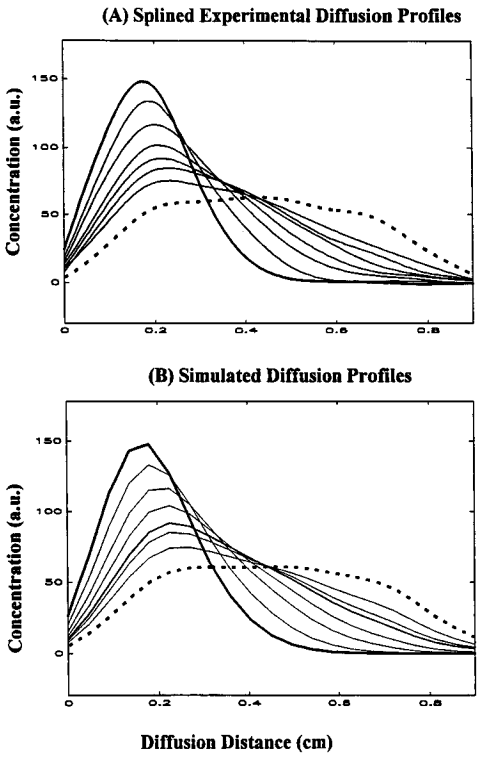

Figure 3. Splined (A) and calculated (B) concentration profiles for the data shown in Figure 2. The abscissa is the length of the sample tube.

manner are shown in Figure 3A for the diffusion of PDTEMPONE in PS30/toluene at 305 K. This type of data was obtained for each of the tracer−polymer systems studied.

Determination of Diffusion Coefficients. The diffusion coefficients D were determined by comparing the experimental splined concentration profiles (such as those shown in Figure 3A) with calculated profiles obtained on the basis of Fick's laws of diffusion.[35] The diffusant is initially confined in the region $0 < x < h$, and the spin probes diffuse into a finite system of length l. The boundary conditions at $t = 0$ are $C = C_0$ for $x \leq h$ and $C = 0$ for $x > h$. An additional condition is $\delta C/\delta x = 0$ at $x = l$ (no flow of the diffusion substance through the closed part of the tube). The solution for this sample configuration is given in eq 1,

$$C(x,t) = \frac{1}{2}C_0 \sum_{n=-\infty}^{+\infty} \left\{ \mathrm{erf}\frac{h + 2nl - x}{2\sqrt{Dt}} + \mathrm{erf}\frac{h - 2nl + x}{2\sqrt{Dt}} \right\} \quad (1)$$

where

$$\mathrm{erf}(x) \equiv \frac{2}{\sqrt{\pi}} \int_0^x \exp[-\xi^2]\, \mathrm{d}\xi$$

and ξ is a variable used in the definition of the error function erf(x). For each time-dependent concentration profile, 21 equidistant points were calculated using eq 1, and five terms ($n = -2, ..., 2$) in the summation were needed for convergence. The sensitivity profile of the ESR cavity along the vertical direction was taken in consideration by multiplying the simulated profiles by the final experimental concentration profile of the sample, measured when a homogeneous distribution of the diffusant in the sample was reached. The three parameters D, h, and C_0 were varied for each experimental profile, until the best fit was reached. In practice, the thickness of the initial layer of the diffusant, h, was determined by simulating the profiles taken in the earliest stage of diffusion; the h value was then kept constant when simulating all profiles for a given sample. The initial concentration was slightly varied in some cases, due to the uncertainty in splining experimental concentration profiles. The typical range of C_0 values used for the simulation of the concentration profiles for a given sample depends on the sample length; for samples ≤8 mm long, the typical C_0 range was ∓4%, while for a sample length of 9 mm the range was ∓10%. In Figure 3B we present the simulated concentration profiles for the diffusion of PDTEMPONE in PS30/toluene at 305 K, which are in excellent agreement with the experimental splined profiles given in Figure 3A.

Each simulated concentration profile gives a value for the diffusion coefficient D. The number of D values for a given system is therefore equal to the number of images, typically 6−10. The diffusion coefficients were deduced as an average of all values determined by fitting profiles of a series taken for the sample in the entire diffusion time range; the experimental error was estimated to be about ±15%.

The diffusion coefficients D of PDTEMPONE in PS solutions in toluene and DMF and in cPS swollen by both solvents are given in Table 1. Data in DMF are limited, for the following reasons. First, the 50 w/w % PS solution in DMF became a gel in the presence of the tracer, suggesting the presence of specific interactions. Second, the diffusion processes of PDTEMPONE in cPS20, cPS25, and cPS50 swollen by DMF were too slow to be measured by spatial−spectral ESRI. For this reasons, we will focus our discussion on systems swollen by, and dissolved in, toluene. The sample cPS05 does not exhibit network properties in toluene because of the high swelling factor and has been excluded from the discussion.

Effect of Polymer Content. Inspection of the D values given in Table 1 indicates that, as expected, the diffusion coefficients of PDTEMPONE in PS solutions decrease with increasing PS concentration and with decreasing temperature. In addition, the values of D at 300 K in cPS networks swollen by toluene are significantly lower that those measured in the solutions at similar polymer content w_2. For instance, D for PS30 (30 w/w % polymer) is larger by a factor of 10 compared to the value for a similar polymer content in cPS swollen by toluene (28.5 w/w %), 4.0×10^{-6} vs 0.4×10^{-6} cm^2 s^{-1}, and similar to the value of D measured for cPS10 swollen by toluene, which contains only 14.9 w/w % polymer. The presence of fixed obstacles to diffusion due to cross-linking is clearly responsible for the difference. The significant decrease of the D values on cross-linking occurs even though the polymer segment between cross-links is larger than the size of the diffusant, as clearly seen in the $M_{x,\mathrm{stoich}}$ values given in Table 1. The glass transition temperatures of cPS samples were measured by differential scanning calorimetry (DSC), and the average number of atoms in the polymer backbone between cross-links, n_x, was estimated using $T_g = T_g^0 + 788/n_x$,[36] where T_g^0 and T_g are respectively the glass transition temperatures of uncross-linked and cross-linked PS. The M_{x,T_g} values evaluated from these measurements are larger by a factor of 2.5−4 compared to $M_{x,\mathrm{stoich}}$, suggesting that the mesh size is larger than that calculated from the DVB content.

The dependence of the diffusion coefficient of small diffusants on the polymer concentration in solution has been often found to follow the free volume theories,[7,37,38] which for polymer concentration lower than ≈50 wt % result in a simple expression, eq 2,

$$\log(D/D_0) = Aw_2/(1 - w_2) \quad (2)$$

where D_0 is the diffusion coefficient in the absence of polymer,

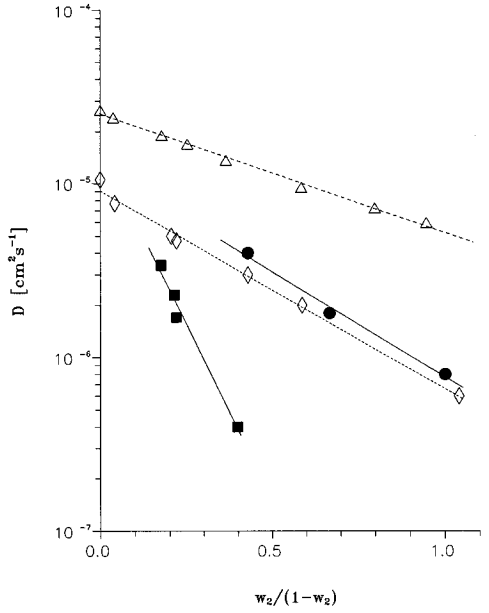

Figure 4. Dependence of translational diffusion coefficients for PDTEMPONE on the polymer content in PS/toluene solutions (●) and in cPS networks swollen by toluene (■) at 300 K. Data for the self-diffusion of toluene in PS/toluene determined by PFGSE NMR[13] at 298 K (△), and for the "dimer" M_2 of styrene in PS/benzene (◊)[11] are given for comparison. Full and dashed lines represent linear fits to the experimental data.

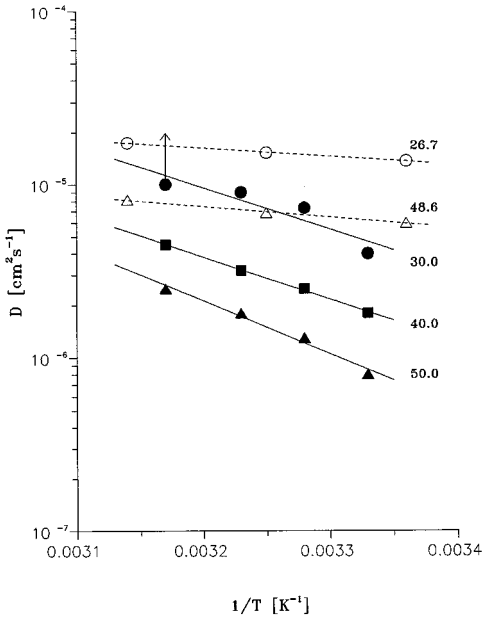

Figure 5. Arrhenius plots of the translational diffusion coefficients for PDTEMPONE in PS/toluene containing 30 (●), 40 (■), and 50 w/w % (▲) polymer. Data for self-diffusion of toluene in PS/toluene for polymer contents of 26.7 (○) and 48.6 w/w % (△) are given for comparison.[13] Full and dashed lines represent linear fits to the experimental data.

A is a system-dependent constant, and w_2 is the weight fraction of the polymer. Plots of log D for PDTEMPONE determined at 300 K vs $w_2/(1 - w_2)$ in toluene solutions of PS and in cPS networks are presented in Figure 4 and fit the linear dependence well.

The data obtained in this study will be compared with two types of data, which are also shown in Figure 4: data for the self-diffusion of toluene in the presence of PS (MW 270 000) at 298 K determined by PFGSE NMR[13] and those for the diffusion of M_2, a "dimer" of styrene, 1,3-diphenyl-1-butanol (MW 226) in PS/benzene at the same temperature.[11] The diffusion coefficients observed for PDTEMPONE and M_2 are very close; the slightly lower diffusion coefficient for M_2 is probably due to both the higher molecular weight of M_2 and the higher viscosity of benzene compared to that of toluene. In contrast, the diffusion of toluene in the PS/toluene binary system is considerably higher than for PDTEMPONE in the ternary system, at comparable polymer content.

The intercept of the data for PDTEMPONE in PS solutions is $\approx 1.3 \times 10^{-5}$ cm^2 s^{-1}, and that for the cPS systems is $\approx 1.6 \times 10^{-5}$ cm^2 s^{-1}; the average, close to 1.4×10^{-5} cm^2 s^{-1}, represents the diffusion of the spin probe in toluene at 300 K. By comparison, the intercept of the data for self-diffusion of toluene in PS/toluene is 2.5×10^{-5} cm^2 s^{-1}, and for M_2 in PS/benzene is 0.9×10^{-5} cm^2 s^{-1}.

The observed effect of cross-linking is in agreement with qualitative observations of solvent penetration into cPS: Both swelling experiments for a series of cross-linked PS by different solvents[39] and NMR imaging studies of dioxane penetration in cPS as a function of the degree of cross-linking[21] have indicated that the transport of solvents in cPS becomes slower with increasing degree of cross-linking.

In contrast to our results and to those mentioned above,[21,39] some studies have suggested similar diffusion rates in polymer solutions and in swollen networks with the same polymer content: A PFGSE NMR study of the diffusion coefficients of toluene in cross-linked PS beads (DVB in the range 5.7−40%) swollen by toluene has detected no measurable differences compared to PS solutions in toluene containing a similar polymer content.[40] The diffusion coefficients for the gels and solutions are close to the newer data published by the same group[13] and presented here in Figure 4. We are unable to explain the discrepancy at this time. We note, however, a significant difference between the swelling ratios (and consequently polymer content) of networks cross-linked in the presence of about 5% DVB, 2.1 for the beads and 4.03 for our cPS gels. The different swelling ratios suggest significant morphological differences between the two types of samples, probably as a result of the different ways of preparation, suspension vs block copolymerization. Obviously, more experimental data on the diffusion rates of tracers, preferably by various techniques, on carefully characterized samples are needed. We believe that in general the diffusion coefficients of tracers depend not only on the network content but also on the degree of cross-linking, molecular mass of diffusant, flexibility of polymer chains, morphology and homogeneity of the medium, and probe−polymer and solvent−polymer interactions.

Johansson et al. have published an extensive study of the diffusion radioactive-labeled monodisperse fractions of poly(ethylene oxide) in polysaccharide solutions and gels, using a scintillation technique.[41] This study has detected no significant differences in the D/D_0 ratios for gels and solutions containing up to 3% polysaccharide. The authors have suggested, however, that the differences in the ratio D/D_0 for gels and solutions containing the same fraction of polymer might be more pronounced for larger diffusants and higher degrees of cross-linking and that the D/D_0 ratio may also depend on the chain flexibility.

Effect of Temperature and Solvent. The temperature dependence of diffusion coefficients is often discussed in terms of an Arrhenius energy of activation. Plots of the diffusion coefficients for PDTEMPONE as tracer in PS/toluene, which are given Figure 5, follow an Arrhenius behavior very well. The activation energies of tracer diffusion, determined from the

slopes of the corresponding plots, are in the range 52 ± 6 kJ/mol for the three PS concentrations in toluene, with the higher value for PS50. For comparison, we also present in Figure 5 data for toluene self-diffusion in PS solutions[13] with polymer contents of 26.7 and 48.6 w/w %. The reported activation energy is significantly lower (≈15 kJ/mol) for self-diffusion in the binary system compared to the diffusion of the tracer in the ternary system.

Faster diffusion of PDTEMPONE at 300 K in PS30/DMF and PS40/DMF compared to the corrsponding PS solutions in toluene could be due to the lower viscosity of DMF, but differences in the conformations and flexibility of the polymer chains in the two solvents are expected to also play important roles in the transport properties of diffusants. The role of molecular architecture in transport has been clearly demonstrated in a recent comparative study of diffusion for linear and cyclic PEO: the behavior of a linear PEO sample of MW ≈ 6000 was shown to be very similar to the cyclic polymer with MW ≈10 000.[42]

Conclusions

The diffusion coefficients D for a small paramagnetic spin probe (PDTEMPONE) were measured in polystyrene (PS) solutions in toluene and dimethylformamide and in cross-linked polystyrene (cPS) networks swollen by the same solvents, using two-dimensional spatial−spectral electron spin resonance imaging (2D ESRI). The D values were found to depend on the solvent, temperature, and PS concentration in the solutions and also on the degree of cross-linking in the cPS networks. For similar polymer concentrations, the presence of cross-links leads to a significant decrease of the diffusion coefficient. The temperature dependence of the diffusion coefficients fits Arrhenius behavior very well, and their dependence on the concentration of polymer in the solution is consistent with the free volume theory.

Acknowledgment. This research has been supported by NSF Grant DMR-9224972 (Polymers Program) and the US−Czech Science and Technology Program Grant 92064. We are grateful to Dr. J. Labský (IMC Prague) for the synthesis of the deuteriated spin probe used in this study and to the reviewers for their constructive criticism.

References and Notes

(1) Crank, J.; Park, H. S. *Diffusion in Polymers*; Academic Press: New York, 1968.
(2) Vieth, W. R. *Diffusion In and Through Polymers*; Hanser Publishers: Munich, 1991.
(3) *Controlled Drug Delivery*; Robinson, J. R.; Lee, V. H. L., Eds.; Marcel Dekker: New York, 1987.
(4) *Ophtalmic Drug Delivery Systems*; Mitra, A. K., Ed.; Marcel Dekker: New York, 1993.
(5) Phillies, G. D. J. *J. Phys. Chem.* **1989**, *93*, 5029.
(6) Lodge, T. P.; Wheeler, L. M. *Macromolecules* **1986**, *19*, 2983.
(7) Wheeler, L. M.; Lodge, T. P.; Hanley, B.; Tirrell, M. *Macromolecules* **1987**, *20*, 1120.
(8) Furukawa, R.; Arauz-Lara, J. L.; Ware, B. R. *Macromolecules* **1991**, *24*, 599.
(9) Waggoner, R. A.; Blum, F. D.; MacElroy, J. M. D. *Macromolecules* **1993**, *26*, 6841.
(10) Nystrom, B.; Walderhaug, H.; Hansen, F. K. *J. Phys. Chem.* **1993**, *97*, 7752.
(11) Piton, M. C.; Gilbert, R. G.; Chapman, B. E.; Kuchel, P. W. *Macromolecules* **1993**, *26*, 4472.
(12) Bu, Z.; Russo, P. S. *Macromolecules* **1994**, *27*, 1187.
(13) Pickup, S.; Blum, F. D. *Macromolecules* **1989**, *22*, 3961.
(14) de Gennes, P. G. *Scaling Concepts in Polymer Physics;* Cornell University Press: Ithaca, NY, 1979.
(15) Lucas, A. J.; Gibbs, S. J.; Jones, E. W. G.; Peyron, M.; Derbyshire, J. A.; Hall, L. D. *J. Magn. Reson.* **1993**, *A104*, 273.
(16) Snaar, J. E. M.; Van As, H. *J. Magn. Reson.* **1993**, *A102*, 318.
(17) Ilyina, E.; Daragan, V. *Macromolecules* **1994**, *27*, 3759.
(18) Bär, N.-K.; Kärger, J.; Krause, C.; Schmitz, W.; Seiffert, G. *J. Magn. Reson.* **1993**, *A113*, 278.
(19) Balcom, B. J.; Fischer, A. E.; Carpenter, A.; Hall, L. D. *J. Am. Chem. Soc.* **1993**, *115*, 3300.
(20) Rana, M. A.; Koenig, J. L. *Macromolecules* **1994**, *27*, 3727. This paper gives a lucid description of the use of NMRI to study sorption of solvents in complex polymeric systems and lists relevant references.
(21) Ilg, M.; Pfleiderer, B.; Albert, K.; Rapp, W.; Bayer, E. *Macromolecules* **1994**, *27*, 2778.
(22) Valtier, M.; Tekely, P.; Kiéné, L.; Canet, D. *Macromolecules* **1995**, *28*, 4075.
(23) Galtseva, E. U.; Yakimchenko, O. Y.; Lebedev, Y. S. *Chem. Phys. Lett*. **1983**, *99*, 301.
(24) Berliner, L. J.; Fujii, H. *J. Magn. Reson*. **1986**, *69*, 68.
(25) Demsar, F.; Swartz, H. M.; Schara, M. *Magn. Reson. Med. Biol.* **1988**, *1*, 17.
(26) Moscicki, J. K.; Shin, Y. K.; Freed, J. H. In *EPR Imaging and in Vivo EPR*; Eaton, G. R., Eaton, S. S., Ohno, K., Eds.; CRC Press: Boca Raton, FL, 1991; Chapter 19, p 189.
(27) Moscicki, J. K.; Shin, Y. K.; Freed, J. H. *J. Chem. Phys*. **1993**, *98*, 634.
(28) Freed, J. H. *Annu. Rev. Biophys. Biomol. Struct.* **1994**, *23*, 1.
(29) Kweon, S.-C. M.Sc. Thesis, University of Detroit Mercy, 1993.
(30) Kweon, S.-C.; Gao, Z.; Eagle, P.; Schlick, S.; Labský, J.; Pilař, J. *Polym. Prepr. Eng. (Proc. ACS Div. PMSE)* **1994**, *71*, 169.
(31) Schlick, S.; Pilař, J.; Kweon, S.-C.; Vacík, J.; Gao, Z.; Labský, J. *Macromolecules* **1995**, *28*, 5780.
(32) Chiarelli, R.; Rassat, A. *Tetrahedron* **1973**, *29*, 3639.
(33) Maltempo, M. M.; Eaton, S. S.; Eaton, G. R. In *EPR Imaging and in Vivo EPR*; Eaton, G. R., Eaton, S. S., Ohno, K., Eds.; CRC Press: Boca Raton, FL, 1991; Chapter 13, p 135.
(34) Maltempo, M. M.; Eaton, S. S.; Eaton, G. R. *J. Magn. Reson*. **1987**, *72*, 449.
(35) Crank, J. *The Mathematics of Diffusion*; Clarendon Press: Oxford, 1993.
(36) *Encyclopedia of Polymer Science and Engineering;* Mark, H. F., Bikales, N. M., Overberger, C. G., Menges, G., Eds.; Wiley Interscience: New York, 1985−89, Vol. 16, p 108.
(37) Vrentas, J. S.; Duda, J. L.; Ling, H. C. *J. Polym. Sci., Polym. Phys. Ed.* **1985**, *23*, 275.
(38) Vrentas, J. S.; Duda, J. L.; Ling, H. C.; Hou, A. C. *J. Polym. Sci., Polym. Phys. Ed.* **1985**, *23*, 289.
(39) Kim, D.; Caruthers, J. M. Peppas, N. A. *Macromolecules* **1995**, *26*, 1841.
(40) Pickup, S.; Blum, F. D.; Ford, W. T.; Periyasami, M. *J. Am. Chem. Soc.* **1986**, *108*, 3987.
(41) Johansson, L.; Skantze, U.; Löfroth, J.-E. *Macromolecules* **1991**, *24*, 6019.
(42) Griffiths, P. C.; Stilbs, P.; Yu, G. E.; Booth, C. *J. Phys. Chem.* **1995**, *99*, 16752.

JP953507I